

D. Pozo-Vázquez · M. J. Esteban-Parra
F. S. Rodrigo · Y. Castro-Díez

A study of NAO variability and its possible non-linear influences on European surface temperature

Received: 8 April 1999 / Accepted: 19 September 2000

Abstract The relationship between European winter temperature spatial and temporal modes of variability and the North Atlantic Oscillation (NAO) has been studied during the period 1852–1997. Temporal modes of variability of the NAO and temperatures are analysed using wavelet transform. Results show that the NAO presents a strong non-stationary behaviour. The most important feature is the existence of a quasi-periodic oscillation, with a period between 6–10 years and maximum amplitude of eight years, during the periods 1842–1868 and 1964–1994. Between 1875 and 1939 the spectra of the NAO is almost white. The possible relationship between the occurrence of extreme events of the NAO and its spectral behaviour has been analysed. The results indicate that quasi-periodic oscillations in the NAO do not lead to more extreme episodes, but rather that an extreme value of the oscillation is more likely to persist for few years. Particularly energetic modes of coherent variability between temperature and NAO are found between 2–6 years for 1857–1879 and 1978–1984, and between 6–10 years from 1961 to 1991. The relationship between the NAO and temperatures as a function of the state of the oscillation has been studied using composites. Empirical evidence has been found suggesting that winter temperatures, in a great part of the study area, do not vary in a linear manner with respect to phase and intensity of the NAO. Regions in the study area differ in sensitivity to changes in the NAO. The spatial patterns of variability of the temperatures are found to be independent of the NAO spectra.

1 Introduction

The strong relationship between mean temperature and circulation conditions in the middle troposphere is well known. Climates of different regions at the same latitude can differ markedly, but low-frequency variations (on interannual and longer time scales) in temperature and precipitation tends to occur in large spatial patterns often associated with changes in distinctive circulation phenomena (Trenberth 1995). Among the several modes of low-frequency variability in geopotential heights in the Northern Hemisphere, one of the most important is known as the North Atlantic Oscillation (NAO) (Barnston and Livezey 1987; Wallace and Gutzler 1981). The NAO is characterised by a north-south sea-level pressure dipolar pattern, with one of the centres located over Iceland and the other one approximately over the Azores Islands. This dipolar pattern reflects the strong contrast in meridional pressure over the North Atlantic region. The NAO dipolar pattern presents a pronounced seasonal variation in its intensity, position and shape (Barnston and Livezey 1987; Mächel et al. 1998). Together with this variability in the position and shape of the dipole, the NAO presents a remarkable interannual variability that can be summarised as the existence of two phases. The positive phase of the NAO reflects below-normal heights and pressure across the high latitudes of the North Atlantic, and above-normal heights and pressure over the Central North Atlantic. The negative phase is characterised by opposed anomalies to those that are observed during the positive phase. Both phases of the NAO are associated with basin-wide changes in the intensity and location of the North Atlantic jet stream, storm track and changes in the patterns of zonal and meridional heat and moisture transport from the Atlantic Ocean to the continental areas of Europe. A northward shift of the axis of maximum moisture transport is observed when the NAO is in the positive phase (Hurrell 1995). This, during the positive phase, results in an intensified westerly flow that brings

D. Pozo-Vázquez (✉)
Departamento de Física, E.P.S., Avenida de Madrid 35,
Universidad de Jaén, 23071, Jaén, Spain
e-mail: dpozo@ujaen.es

M. J. Esteban-Parra · Y. Castro-Díez
Departamento de Física Aplicada, University of Granada, Spain
F. S. Rodrigo
Departamento de Física Aplicada, University of Almería, Spain

warm maritime air to Europe during winter, reducing the polar outbreaks over Europe and leading to a warming of Central and Southern Europe and a cooling of the northwestern Atlantic area (van Loon and Rogers 1978; Rogers and van Loon 1979).

Several reports have evaluated the importance of extratropical low-frequency atmospheric circulation variations in determining recently observed decadal-scale temperature shifts in the Northern Hemisphere (see e.g. Trenberth 1990; Wallace et al. 1995). In some cases, changes in the atmospheric circulation can lead to warmer-than-normal temperatures over extensive continental areas and a cooling over the oceans. Calculations of hemispheric temporal averages do not result in cancellations between warm and cool areas, but rather a net warming over the entire region. This is due to the lower heat capacity of the land (Wallace et al. 1996), leading to a dynamically induced variability in temperatures. In this way, changes in the NAO have been found to be partially responsible for the warming over continents at high latitudes (40°N poleward) during the twentieth century. Hurrell (1996) showed that NAO and El-Niño-Southern-Oscillation (ENSO) could account for 44% of the winter temperature variability in the North Atlantic region during the last 60 years, with the NAO constituting the leading factor (33%). The NAO influence on climate persists throughout the year, although it is stronger in winter than in other seasons. This difference in strength is mainly because winter temperature anomalies tend to be determined by regional-scale features, while warm season temperature anomalies tend to have a more uniform (hemispheric) pattern (Wallace et al. 1996). Additionally, the NAO presents the strongest pressure gradients and interannual variability during winter (Moses et al. 1987). According to Palecki and Leathers (1993), 72% of the variation in the January Northern Hemisphere land-surface temperature can be explained on the basis of variations in low-frequency atmospheric circulation, mainly the NAO and the Pacific/North American pattern (PNA). In a recent study, Osborn et al. (1999) studied the relationship between NAO and climate of the Northern Hemisphere using both observed and simulated data from the coupled climate model of the Hadley Centre (HadCM2). Several works have focused on the relationship between large-scale pressure field, as the NAO, and European climate in particular. For instance, Zorita and von Storch (1997), using canonical correlation analysis, identified NAO-like pressure patterns predominating over Europe during winter and producing significant air-temperature changes over Scandinavia (56% explained variance). Werner and von Storch (1993) studied the relationship between the large-scale sea-level pressure field over Europe and temperature in January and February in Central Europe for the period 1901–1980. In all these studies, spatial patterns of temperature variability associated with the NAO are based on the assumption of a linear relationship. In particular, spatial patterns associated with positive and negative phase of

the NAO have been assumed to be the same. Studies with another teleconnections, the ENSO, have shown different spatial patterns of climate variability within its influence zone during positive and negative events (Hoerling et al. 1997).

The aim of the present study is to increase current knowledge of the relation between European winter temperature spatial and temporal modes of variability and the NAO. In particular, the spatial patterns of temperature associated with different phases and intensities of the NAO have been analysed. This should, eventually, elucidate whether or not the relation between winter temperature in Europe and the NAO is linear. We also study the temporal stationarity of the relation between NAO and spatial patterns of winter-temperature variability as well as the influence of the spectral characteristics of the NAO on these spatial patterns.

The study is divided in two parts. In the first part, spatio-temporal patterns of variability of the winter (December through February) temperatures for the period 1852 to 1997 are obtained using principal components analysis (PCA). The area studied includes a great part of the European continent. Wavelet spectrum of the winter NAO index and the principal components series (PCs) are computed and their characteristics are analysed. In the second part, we study the relation between the NAO and the temperatures as a function of the phase and intensity of the oscillation. To do so, we use composites of temperature anomalies to examine the patterns associated with positive and negative phases of the oscillation. Finally, to study the temporal stationarity of the relation between the temperature variability and the NAO, as well as the possible influence of the NAO spectral characteristics, two independent PCAs have been carried out for the periods 1875–1939 and 1940–1997.

Section 2 describes the methodologies used in this study, concerning PCA and the wavelet analysis. Section 3 describes the data used. Section 4 shows the results of the analysis. Finally, a discussion of the results and some conclusions are provided in Sect. 5.

2 Methodology

The PCA (Preisendorfer 1988; von Storch 1995) is used to obtain the general spatio-temporal characteristics of temperature variability in Europe. To achieve physically meaningful patterns and a better comprehension of them, we rotated the empirical orthogonal functions (EOFs) using the varimax method (Richman 1986). This is the most widely used rotation technique and has been shown to produce statistically stable patterns (Cheng et al. 1995). Although several techniques have been proposed, there is no general agreement in the criteria to select the significant EOFs to rotate. In this study, the number of significant EOFs was chosen using the selection rule of North et al. (1982). Rotation was applied using several subsets of EOFs around the number indicated by the North rule, in order to test the importance of the number of rotated EOFs in the results. No significant differences were found. The rotated EOFs (REOFs) found represent spatial patterns of temperature variability and their associated PC time series provide a concise way of monitoring the climate.

Composite analysis is used to examine the patterns associated with the different phases of the oscillation. This analysis consists of a sampling procedure; temperature time series at each grid are sampled based on the state of the NAO and mean values (composites) are computed for each of the resulting time series. The Student's *t*-statistic is also computed at each grid to check the statistical significance of the difference between means resulting from different NAO states. A signal will be considered significant if it is significant at the 95% level for a two-tailed test of the null hypothesis of no difference between means. The test takes into account that the two samples come from populations that may have unequal variances and that the number of data in each sample may be different (Canovas 1988; ch9). Composite analysis has been widely used in previous studies, particularly in the search for teleconnections related to the ENSO (Kiladis and Diaz 1989; Hoerling et al. 1997; Huang et al. 1998).

To complete the composite analysis, we have examined the consistency among events of the relationship between the NAO and temperatures. The magnitude of anomalies (selected as a function of the state of the NAO) can vary between events (even with the same state of the NAO), and this could lead to composites dominated by a few major anomalies. It is thus necessary to ascertain the extent to which the signal at a given place is consistent among events. We have addressed this problem by calculating the percentage of consistent signals (or coherence), defined as the percentage of events having a temperature anomaly of the same sign that the composite anomaly.

Climatological time series constitute one of the key tools for understanding climate. These series reflect the variability of the climate system and its underlying dynamic, which, in most cases, is chaotic (Lorenz 1997). Consequently, many climatic time series have non-stationary behaviour, presenting, from a spectral standpoint, transient components. These components excite a wide range of frequencies in a limited amount of time. Methods of standard time-series analysis, in order to provide a time or spectral-domain representation of the main characteristics of a time series, rest on the simplifying assumption that the series under study, or certain simple transformation of it, is stationary. That is, the mean and variance are constant through the time series and the autocorrelation function (ACF) depends only on the time lag. Classical spectral and cross-spectral analysis, based on Fourier transform (FT), is not the most suitable tool for the analysis of non-stationary time series and the study of their relationships. This is mainly because Fourier transform does not contain any time dependence of the signal and therefore cannot provide any local information regarding the time evolution of its spectra. Furthermore, sine and cosine functions used in the FT are defined endlessly in time, so that possible singularities in a time series are spread over the entire power spectrum, creating spurious peaks and cancellations of real ones.

Recently, a newly developed technique called wavelet transform (Kaiser 1994) has been applied to the study of climatic and geophysical time series in general. Wavelet analysis is a powerful non-linear tool for time-series analysis: by breaking down a time series into time-frequency space, wavelet analysis indicates both the dominant modes of variability in our time series and how these modes vary over time. Wavelet analysis has been used in numerous climatic studies: Wang and Wang (1996) used wavelet transform to study the temporal structure of the Southern Oscillation; Huang et al. (1998) used cross-spectral analysis based on the wavelet transform to study the relationship between the NAO and the ENSO. An introduction to the wavelet analysis concerning climate can be found in Lau and Weng (1995) and a review of the applications of wavelet analysis in geophysics is given in Fofoula-Georgiou and Kumar (1995). In Yiou et al. (1996) a comprehensive review of spectral techniques for climatic data analysis, particularly the wavelet analysis, and their main properties and pitfalls can be found, while Torrence and Compo (1998) recently published a comprehensive and practical guide to wavelet analysis.

In the present study, Morlet basis function has been used to determine the wavelet power spectrum of the NAO and the temperature PC series and cross-wavelet spectrum between NAO and temperature time series. Normalisation of the wavelet power

spectrum and cross-wavelet power has been carried out using the variance of the series. Such normalisation gives a measure of the power relative to white noise (the expectation value of the wavelet power spectrum of a white noise process is one at all periods and time). Wavelet power spectrum can be tested against a red-noise background process with a lag-1 coefficient ϕ_1 , in which $\phi_1 = (\alpha_1 + (\alpha_2)^{1/2})/2$, being α_1 and α_2 the lag-1 and lag-2 autocorrelation of the time series under study. Confidence intervals can be obtained based on the χ^2_2 distribution multiplying the background red noise spectrum by the 95th percentile value for χ^2_2 . In the same way confidence intervals can be obtained for the cross-wavelet spectrum (for a more complete description see Torrence and Compo 1998). The global wavelet power spectrum has been also computed for each series. This is the time-mean wavelet spectrum determined by averaging the wavelet transform coefficient over the period analysed. Percival (1995) shows that the global wavelet spectrum provides an unbiased and consistent estimation of the true Fourier spectrum of a series.

3 Data

Gridded winter air-temperature data from 1852 to 1997 of the North Atlantic land regions, comprising Western, Central and Southern Europe, Southern Scandinavia, and North Africa (Latitude 35°N to 60°N; Longitude 10°W to 20°E), has been analysed. The data (provided by the Climatic Research Unit, University of East Anglia, UK) are defined on a 5° latitude by 5° longitude grid-box basis and are expressed as anomalies from the corresponding monthly averaged values of the period 1961–90 (Jones 1994). The dataset has been extensively used, Parker et al. (1994) and in the last IPCC report (Nicholls et al. 1996). Winter temperatures (December, January, and February) were determined by averaging the corresponding values monthly values. The influence of NAO on temperature covers a greater area than the one that we have used (Hurrell 1996; Osborn et al. 1999). A key issue in the present work is the existence of long series, given that we have to establish several subsets of each series. Outside of the selected area, many gaps in the data were found throughout the period 1852–1997 and the analysis would be biased when comparing results from different subsets. Only a few series over an area northwest of the British Isles, over Sicily and over Northern Africa, have missing data, especially during the first few decades. Missing data have a zero value. The standard error due to sampling of the individual values since 1951 is estimated to be 0.05 °C (Jones et al. 1997a).

The winter (December to February) index representative of the NAO, from 1826 to 1997, developed by Jones et al. (1997b), has been used. The index was formulated using pressure data from Gibraltar (36.1°N, 5.4°W) and Iceland, the latter computed mainly using data from Reykjavik (64.1°N, 22.9°W). In particular, among the stations available during the winter, Gibraltar appears to represent the southern part of the NAO dipole better than do other stations (Lisbon and Ponta Delgada in the Azores) (Pozo-Vázquez et al. 2000; Jones et al. 1997b). Due to the different statistical characteristics of the pressure data from the northern and southern stations (especially regarding the standard deviation), and due to the change of both mean and standard deviations through the year, a normalisation process for each pressure time series is necessary to prevent the index being biased and misleading. Thus, a monthly deseasonalised and normalised index was constructed for each station. This method consists of calculating the difference between each raw monthly value and a time-averaged monthly mean value, and then dividing by a time-averaged monthly standard deviation. Normalisation relative to the period 1951–1980 was used. Although other normalisation procedures have been proposed (Ropelewski and Jones 1987), this has been argued to be optimal (Trenberth 1984). The winter index has been computed by averaging the monthly indices. Due to the selected normalisation period, the NAO winter index does not have mean zero and standard deviation unity. Throughout this work, several analyses are made with subsets of data selected as a function of the NAO index value.

In particular, values $|\text{NAO}| \leq 1.5$ are considered to be near normal or moderate NAO index. Values of the NAO index $1.5 < |\text{NAO}|$ are considered to be extreme events. These threshold values were empirically determined, based on the analysis of the NAO winter index time series while taking into account the length of the data record available.

4 Analysis

4.1 PCA of the winter temperature: 1852–1997

EOFs were calculated for the entire data set (1852 to 1997). Four significant EOFs were found and varimax rotation was applied. The four significant REOFs account for 76.6% of the total variance. Figure 1 shows the corresponding spatial patterns by drawing the isolines of the loading factors. The leading mode (Fig. 1a) explains 38.1% of the variance. Figure 2a shows the corresponding PC series and the NAO index. The correlation coefficient between the two series is 0.8 (statistically significant). Figure 1a shows that this mode of variability is especially strong over the British Isles,

Western and Central Europe and Southern Scandinavia, in which loading factors reach values higher than 0.8. This pattern is less representative of the variability over Southern Europe, reaching loading factors smaller than 0.2 over the Iberian and Southern Italian Peninsulas. Other authors have reported similar patterns as the spatial signature of the NAO on the temperature over the studied area (see e.g. Hurrell 1996; Osborn et al., 1999).

The Mann-Kendall (Sneyers 1992) and Pettit (Pettit 1979) tests have been computed to check the presence of trends in the period analysed and to find the time of onset and end of these trends. For the case of the NAO index (Fig. 2a), the Mann-Kendall test shows a statistically significant upward trend from 1902 to 1925. A simple linear fit for this period results in a trend of 0.20^* units/decade (* indicates statistical significance at 95% confidence level). In the analysis of the PC associated with the first REOF (Fig. 2a), similar results are found. The Mann-Kendall test shows evidence for a significant trend between 1897 and 1927, with a value of 0.28^* degrees/decade. The Pettit test globally confirms these features in both series. Finally, although both the PC

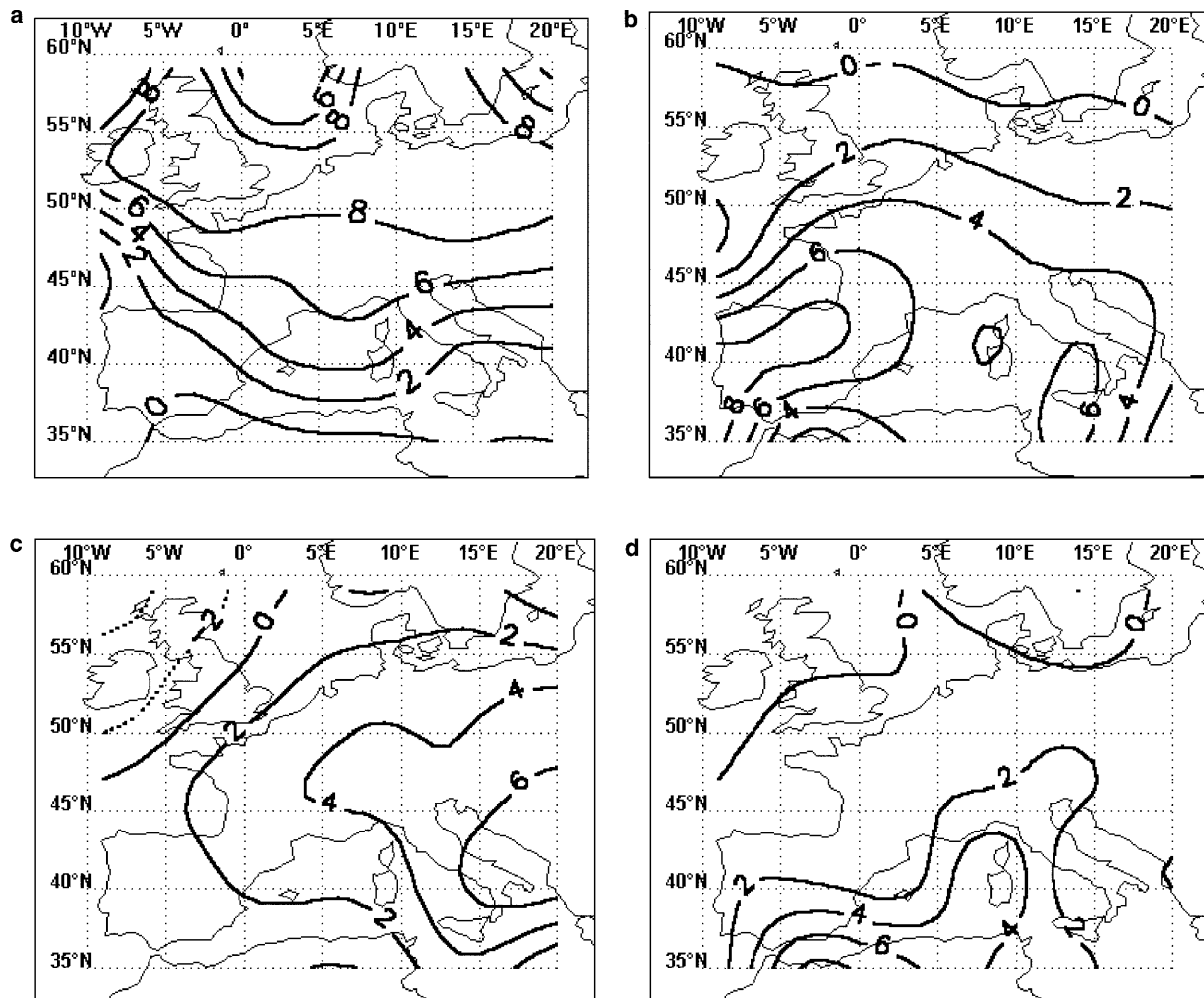


Fig. 1a–d Loading factors (by ten) for the a first, b second, c third and d fourth REOF resulting from the analysis of the winter temperatures during the period 1852–1997. *Continuous line* indicates positive or zero loading and *dotted line* indicates negative loading

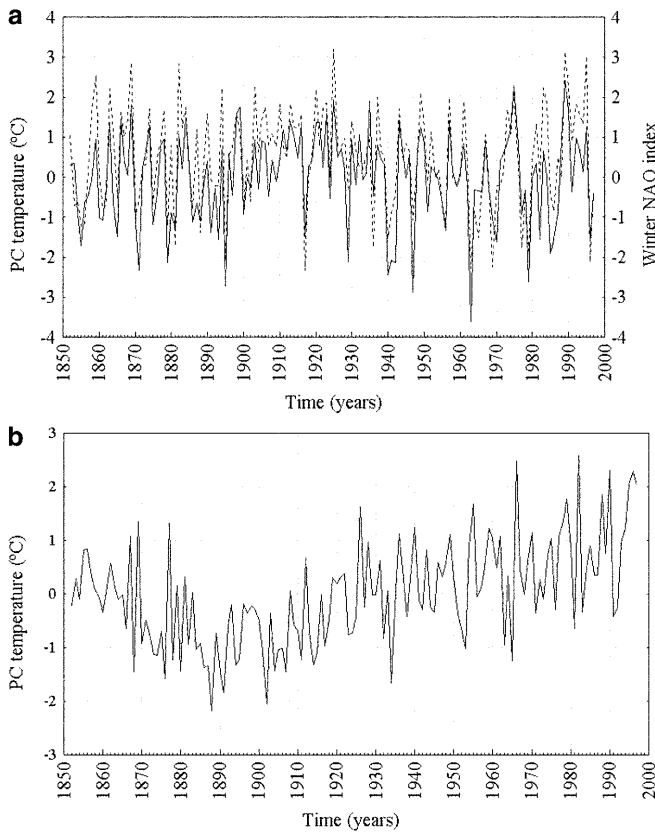


Fig. 2a, b PC series corresponding to the **a** first and **b** second REOF resulting from the analysis of the winter temperature in the period 1852–1997. Units are °C (anomalies). For the first PC, the NAO winter index is also shown (*dashed line*)

series associated with the first REOF, and the NAO, index visually show a steep positive trend from 1980 to 1995, no statistical significance for this trend can be achieved using the Mann-Kendall and Pettit test.

Figure 1b shows the pattern of spatial variability associated with the second REOF, which explains 20% of the total variance, and Fig. 2b shows the corresponding PC series. This mode is representative mainly of the variability over southwestern Europe, especially over the Iberian Peninsula (where loading factors greater than 0.8 can be found). Correlation with the NAO index is 0.06 (non-statistically significant). The Mann-Kendall and Pettit test shows the presence of two statistically significant trends. The first is a downward trend during the decade 1852–1891, with a value of -0.45 degrees/decade. The second is an upward trend from 1918 to the end of the series, with a value of 0.15 degrees/decade. Esteban-Parra (1995) found the same trend in an independent study of climatic variability in the Iberian Peninsula. Figure 1c, d shows the patterns associated with the third and fourth REOFs. These patterns are of less importance in explaining the total variability and are representative mainly of the variability of the southeastern part of Europe and North Africa. The correlation between the corresponding PC series and the NAO index are negligible.

4.2 Wavelet analysis

In this section, we conduct a wavelet analysis of the NAO time-series index and the temperature PC series. This analysis provides the modes of temporal variability of the NAO and PC temperature series and how these modes have changed through the period analysed. Furthermore, the comparison of the results can provide information on the relationship between temperature and NAO.

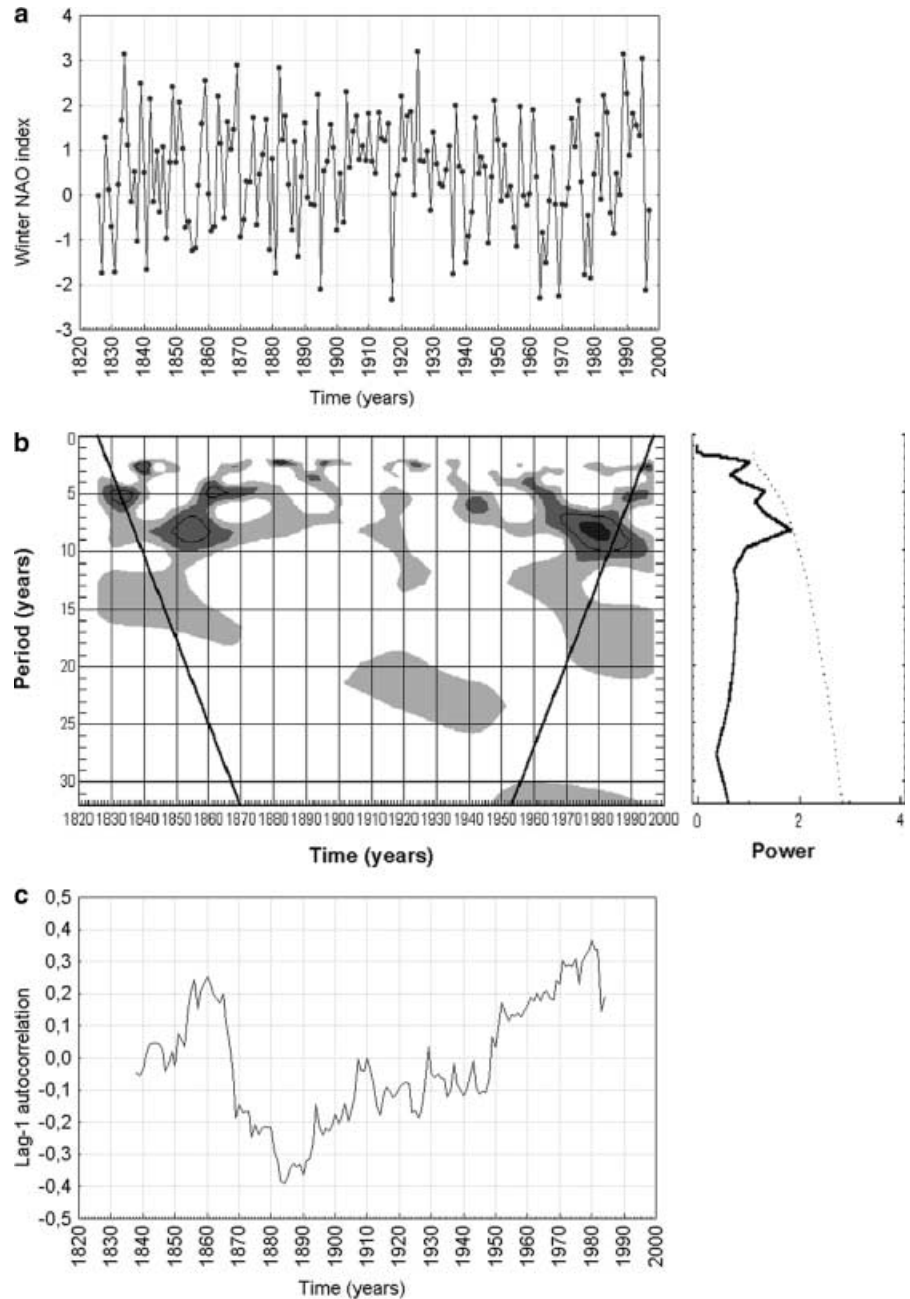
4.2.1 NAO index

Figure 3a shows the winter NAO index variability, from 1826 to 1997, used in the wavelet analysis. Figure 3b (left) shows the wavelet power spectrum of the winter NAO index displayed as a function of period and time. The left axis is the Fourier period; the bottom axis shows the time in years. Figure 3b (right) shows the global wavelet power spectrum.

The strongly non-stationary behaviour of the spectra is clearly seen, there is no evidence for a single persistent temporal mode of variability in the NAO index in the time interval 1826–1997. Power is concentrated in periods of less than 10 years, mainly between 6–10 years and with less importance in 2–6 years. The amplitude and strength of the modes of variability change dramatically with time. A statistically significant and very energetic oscillation with period between of 6–10 years and maximum amplitude in an 8-year period appears at the beginning of the record, between 1842 and 1868. This oscillation suddenly vanishes and the behaviour of the NAO until 1940 closely resembles that of a white-noise process. Some oscillations, of weak energy and statistically non-significant, are found having periods between 10–15 and 15–20 years. These appear almost in the same periods undergoing oscillation between 6–10 years. Around 1964, again, a highly energetic oscillation (statistically significant) began, with a period between 6–10 years and maximum amplitude at 8 years, and this reached its maximum amplitude between 1974 and 1984. This oscillation tended to disappear in the late nineties, although the proximity of the end of the record reduces confidence in this conclusion. In the band of 4–6 years, relatively strong power appears, especially at the beginning of the record, between 1857 and 1875, between 1939 and 1946 and between 1956 and 1966. In a recent study, Huang et al. (1998) found significant modes of coherent variability between ENSO and the NAO in this band for the same time periods. Throughout the entire record, there are short episodes of quasi-biennial oscillation, statistically significant but lasting a very short time. This quasi-biennial oscillation predominates during the period 1880–1890. Figure 3b (right) shows that, when integrating wavelet spectrum, statistical significance is lost for the whole period.

Several studies have analysed the spectral characteristic of the NAO index. Rogers (1984) analysed the Fourier spectrum of the NAO winter index from 1900–

Fig. 3 **a** NAO winter index from 1826 to 1997. **b** (Left) wavelet power spectrum of the winter NAO index displayed as a function of period and time. Shaded contours are at normalised variances 2, 5 and 10. Regions of greater than 95% confidence level for a red-noise background spectrum with a lag-1 coefficient $\phi_1 = 0.1$ are enclosed by a thick contour. Regions below the thick diagonal line at both ends indicate regions where the edge effects due to the finite length of the series are important and results are not reliable. **b** (Right) global wavelet power spectrum. Normalisation is to variance 1, the dashed line is the 95% confidence level for a background red noise spectrum with lag-1 autocorrelation 0.1. **c** Lag-1 autocorrelation of the NAO winter index calculated using a sliding window spanning 25 years



1883, using pressure data from Iceland and the Azores, finding pronounced peaks at periods 5, 7 and 20 years. Hurrell and van Loon (1997) reported the Fourier power spectrum of winter NAO index from 1865 to 1997, identifying peaks at periods 2–3 and 6–10 years and inter-decadal bands. They also found a trend of the NAO spectra to become redder with time. These results globally confirm our findings, especially when compared with the global wavelet spectrum. In a recent study, Appenzeller et al. (1998) used wavelet transform to analyse a proxy NAO annual index of 350 years and an annual instrumental index, developed by Hurrell (1995), covering the period 1865–1997. They found highly non-stationary behaviour in the NAO index and discovered that the maximum power is concentrated in periods

of less than 15 years (as in our analysis, although we analyse winter data).

Additional information of the stationarity of the NAO index can be achieved studying its autocorrelation. Figure 3c shows the lag-one autocorrelation of the NAO winter index calculated over a sliding window spanning 25 years. When we take into account the entire series, the NAO winter index closely resembles a white-noise process, its lag-1 autocorrelation value being 0.11. This means that there is almost no relationship between the value of the index of one winter and the value of the preceding winter. Nevertheless, Fig. 3c shows that the lag-1 autocorrelation value is far from stationary in time. Between approximately 1850 and 1865, the lag-1 autocorrelation has a value around 0.2, similar to values

at the end of the record. Perhaps the most striking feature in Fig. 3c is the steep change in the lag-1 autocorrelation value, including a change of sign, roughly between 1865 and 1885. During this relatively short period, the lag-1 auto-correlation changes from a positive value of 0.2 (that is, some degree of persistence) to a -0.4 value (indicating the predominance of a biennial oscillation, in which the current value of the index is negatively correlate with the preceding one). Another important feature in Fig. 3b, c is that the low-frequency signal in the NAO index strengthened in the late part of the twentieth century compared with the first part but not compared with the period 1840–70.

The non-stationary behaviour of the NAO spectra raises a question concerning whether or not the occurrence of extreme events of the oscillation are in some way linked with the spectral behaviour of the NAO. A simple inspection of the NAO index (Fig. 3a) reveals that there have been some time-intervals in the period 1875–1939 with few extreme values of the NAO ($|\text{NAO}| > 1.5$). For instance, in the period 1900–1910 three extreme values are found and also three in the period 1925–1939 (including the period 1926–1935 with no extreme values). However, when we take into account longer periods, we find extreme values of the NAO almost equally distributed over the entire dataset. During the period 1875–1939 (in which spectral behaviour of NAO resembles white noise) the numbers of extreme episodes of the NAO were 20 and 19 during the period 1940–1997 (in which oscillations in the band of the 6 to 10 year period predominates). The different spectral behaviour during these two periods appears not to have exerted any major effect on the number of extreme values of the NAO. The only effect is that the occurrence of extreme episodes of the NAO is completely random in the period 1875–1939 compared with the period 1940–1997, in which inter-decadal variability predominates in the behaviour of the NAO. The appearance of quasi-periodic oscillations does not lead to more extreme episodes of the oscillation, but rather persistence at an extreme value of the oscillation is more likely for few years. These episodes of persistence can be found, for instance, in the periods 1973–1975, 1983–1984 and also in the period 1989–1995, with five of the seven winters having a value of the NAO > 1.5 . Similar episodes of persistence can also be found from 1853 to 1856.

4.2.2 Temperature PC series

Wavelet power spectrum has been computed for the PC series corresponding to the leading and second REOF found in the analysis of the entire data set 1852–1997. Figure 4a (left) shows the results for the leading REOF. The non-stationary behaviour found for the PC series is notable; its characteristics closely resemble those found in the wavelet analysis of the NAO index. An energetic (and statistically significant) oscillation of periods in the band of 6–10 years and maximum amplitude at 8 years

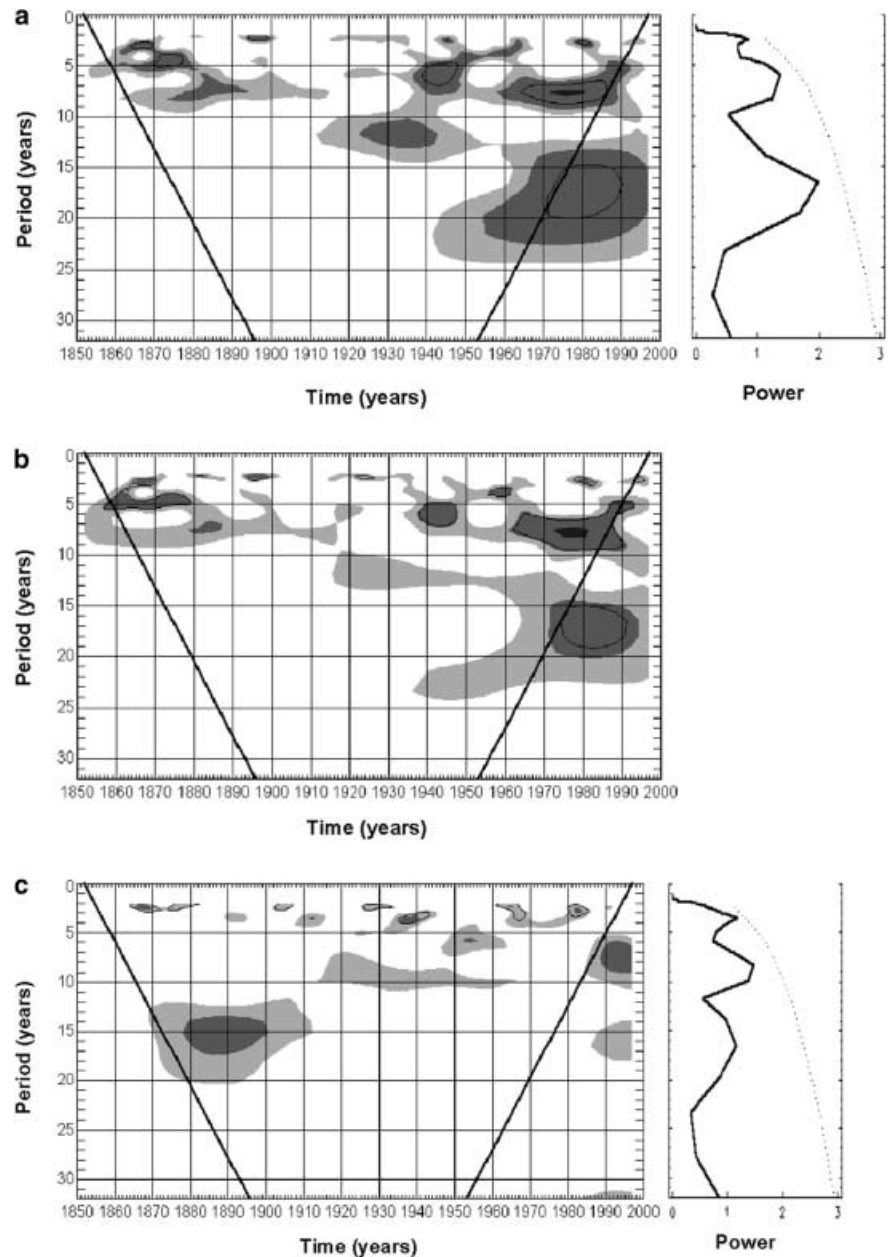
appears between 1958 and 1992 and reaches its maximum amplitude between 1972 and 1981 (very similar to the NAO spectra). Valuable power in this band also appears between 1873 and 1893. Statistically significant power is found at period of 15–20 years from 1955 onwards, although reliability of these results is constrained by the influence of the end of the series (cone of influence). In the band of 4–6 years, statistically significant power can be found between 1870 and 1877 and between 1939 and 1948. Between 1894 and 1900 and between 1977 and 1983, a statistical quasi-biennial oscillation is found. Figure 4b shows the cross-wavelet power spectrum for the PC of the leading REOF and the NAO index. Substantial covariance (statistically significant) is found to be associated with periods in the band of 5–10 years for the time interval 1961–1993; in the band of 4–6 years, between 1857 and 1879 and in the band of 5–8 years between 1937 and 1947. Statistically significant covariance is also found for quasi-biennial periods in some short time intervals, such as in 1894–1900 and 1977–1983. From 1972 to 1995, there is a region of statistically significant covariance in the band of 15–20 year periods, although the influence of the end of the series lessens the reliability of the results in this region.

Since Fig. 4b indicates that the regions of maximum covariance are found in periods of 2–10 years, we carried out an additional analysis in this band. Figure 5a shows the integrated wavelet power spectrum in the band of 2–6 year periods, for the NAO index (solid line) and the temperature PC series (broken line). Figure 5b shows the same but in the band of 6–10 years. The comparison of the variance amplitudes of NAO and temperature PC series in the band of 2–6 years evidences a different behaviour over time. Amplitude is in phase from 1862 to 1878 and from 1975 to 1985 and out of phase from 1878 to 1890 (but of little amplitude for the temperature PC series). For other time periods, a certain lag exists or no coherence at all is found. For instance, during the period 1940–1950, a valuable signal is found in the 2–6 year band for the PC temperature series but not for the NAO. Thus, coherence between temperature and NAO in the band of 2–6 years is confined to the periods 1862–1878 and 1975–1985. In the band of 6–10 years the comparison of the amplitudes of the NAO and the PC series shows, to some degree, a stationary behaviour, being in phase for almost the entire record.

The former analysis suggests that covariance of the PC series and NAO is particularly important in the band of 2–6 years period for the time periods 1857–1879 and 1978–1984, and in the band of 6–10 in the last part of the record (1961–1991).

Figure 4c shows the wavelet power spectrum for the PC series associated with the second REOF. The main feature is a low-frequency oscillation associated with periods between 14–17 years (statistically significant at 90% confidence level during the period 1878–1900). Beyond this pulsation, only some oscillations in the 2–5 year band, which last a short time, are worth noting.

Fig. 4 **a** As in Fig. 3b but for the PC series corresponding to the leading REOF obtained in the analysis of the winter temperatures of the period 1852–1997. A lag-1 coefficient $\phi_1 = 0.1$ has been used. **b** Cross-wavelet power spectrum for the NAO winter index and the PC associated with the leading REOF determined from the analysis of the entire dataset 1852–1997. Shaded contours are at 2, 5 and 10. Statistically significant regions are delineated by a thick contour; the 95% confidence level was derived assuming red-noise background spectrum with lag-1 coefficient $\phi_1 = 0.1$ both for the NAO index and the PC series. **c** As **a** but for the second PC and using $\phi_1 = 0.47$



No resemblance between the characteristics of this spectrum and those of the NAO can be discerned when comparing Figs. 3b and 4c.

4.3 Analysis of subsets of data

4.3.1 Separate NAO index values: composite analysis

In this section, composite patterns of temperature anomalies are determined in order to study the relationship between the NAO and winter temperature as a function of the state of the oscillation. The different composite patterns are determined based on years selected as a function of the value of NAO winter index.

Figure 6a shows the composite of temperature anomalies for years in which the value of NAO index was $NAO > 1.5$ (35 cases); during these years the NAO was in an extremely positive phase. Figure 6b shows the composites for years with $0 < NAO \leq 1.5$ (64 cases); these years are of moderately positive or near normal NAO state. Figure 6c shows the differences, Fig. 6a minus b, between the two patterns. For each grid, a student *t*-test has been computed to check out the significance of the difference between composites. Shaded areas in Fig. 6c indicate local statistical significance at 95% confidence level for the difference in the means. During years with $NAO > 1.5$, maximum positive anomalies, of value $1.5\text{ }^{\circ}\text{C}$, are found over northern Germany and Poland and southern

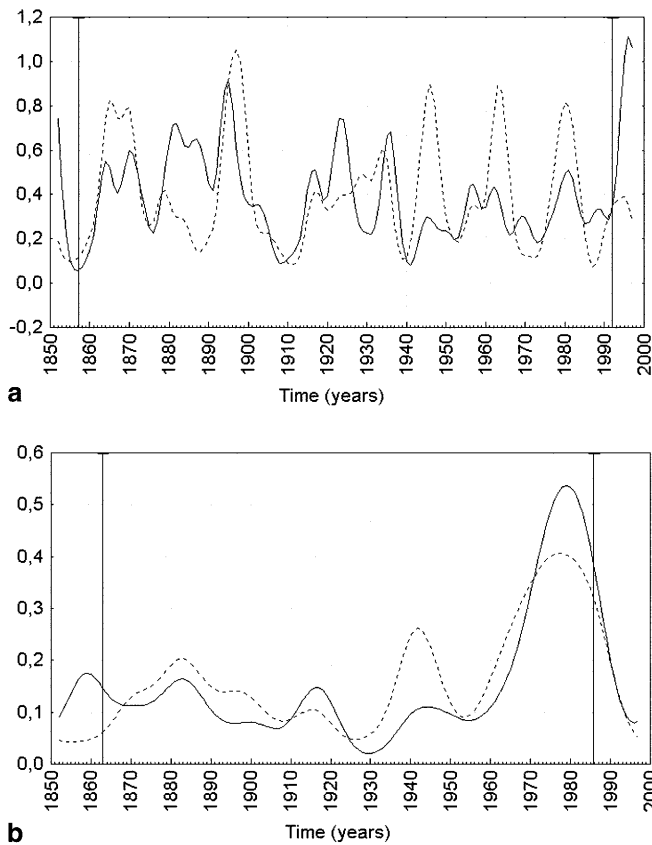


Fig. 5 **a** Integrated wavelet power spectrum in the band of 2–6 year periods of the NAO index (solid line) and the temperature PC series (dashed line). **b** As in **a** but for the band of 6–10 years. The ordinates are units of variance. Vertical lines at the beginning and end of the record indicate regions possibly influenced by the end of the series

Scandinavia. Slightly negative anomalies of value $-0.2\text{ }^{\circ}\text{C}$ are found over the Iberian and the southern Italian peninsulas.

During winters with $0 < \text{NAO} \leq 1.5$, the temperature anomalies have a maximum value of $0.5\text{ }^{\circ}\text{C}$ over northern Germany, southern Scandinavia and the British Isles. Negative anomalies of value $-0.5\text{ }^{\circ}\text{C}$ are found over the Iberian and southern Italian peninsulas. The differences in temperature between extremely positive and moderately positive NAO winters (Fig. 6c) are statistically significant over Western and Central Europe, southern Scandinavia and the British Isles. The greatest differences (more than $1\text{ }^{\circ}\text{C}$) are found over northern Germany and Poland and southern Scandinavia. On the other hand, minor differences (not statistically significant) are found over southern Europe (the Iberian and southern Italian peninsulas). Over this area, temperatures show no significant changes when years with a highly positive NAO are compared against years with a moderately positive NAO. In both cases, anomalies are slightly negative.

The same analysis was made but for negative NAO index values. Figure 6d shows the composite of temperature anomalies during years with extremely negative

NAO, ($\text{NAO} < -1.5$, 10 cases). Figure 6e shows the composite for moderately negative years ($-1.5 \leq \text{NAO} \leq 0$, 37 cases) and Fig. 6f shows the differences (Fig. 6d minus e). In Fig. 6d, strongest negative anomalies (between -1.5 and $-2\text{ }^{\circ}\text{C}$) are found over northern Germany, Poland, southern Scandinavia and the British Isles. Anomalies close to zero are found over the middle of the Iberian and Italian peninsulas, while positive anomalies (of value $0.5\text{ }^{\circ}\text{C}$) are seen over the southern part of Spain and over North Africa. During moderately negative NAO years, over most part of Western and Central Europe anomalies have values of around $-1\text{ }^{\circ}\text{C}$, reaching $-1.5\text{ }^{\circ}\text{C}$ over southern Scandinavia. Over the northern Iberian and southern Italian peninsulas, anomalies of value $-0.5\text{ }^{\circ}\text{C}$ are found. Figure 6f shows that, for most of the study area, anomalies during moderately negative NAO years are similar to those found for strongly negative years. The differences are statistically significant at 95% confidence level only for the very south of the Iberian and Italian peninsulas and Sicily, where differences are positive. Differences are also statistically significant but negative over Ireland and northern Britain.

Finally, the consistency among events of the relationship between the NAO and temperatures was examined by calculating the percentage of consistent signals. Figure 7a shows the percentage of coherence during extremely positive NAO, Fig. 7b for moderately positive, Fig. 7c for extremely negative NAO, and Fig. 7d for moderately negative. Sharply different values of consistency are found in the study area. During extremely positive NAO, consistency exceeded 80% over most part of Western and Central Europe, reaching values up to 100% over the British Isles and southern Scandinavia. Values of 60% (mainly related to climatology) are found over the Iberian and Italian peninsulas. During moderately positive NAO, values of 80% integrated wavelet power spectrum in the band of 2–6 year periods are found over the north of the British Isles and southern Scandinavia (Fig. 7b), a remarkable value with respect to the coherence in the extremely positive phase. This reduction also occurs over most of Western and Central Europe, where values are around 60%. The western Iberian Peninsula shows a value of 80%, greater than the value found in the extremely positive NAO. This agrees with the fact (Fig. 6a, b) that during moderately positive NAO the composite values are greater in amplitude ($-0.5\text{ }^{\circ}\text{C}$) than during extremely positive ($-0.2\text{ }^{\circ}\text{C}$).

The analysis of the extremely negative phase of the NAO (Fig. 7c) shows a 100% value only over the northern part of the British Isles, while over southern Scandinavia, values are between 70% and 80%. During moderately negative NAO events (Fig. 7d) the percentage of coherence over these two areas remains substantially the same found in the analysis of the moderately positive NAO. Furthermore, when comparing Fig. 7c and d, the percent of coherence do not change substantially over Central and Western Europe

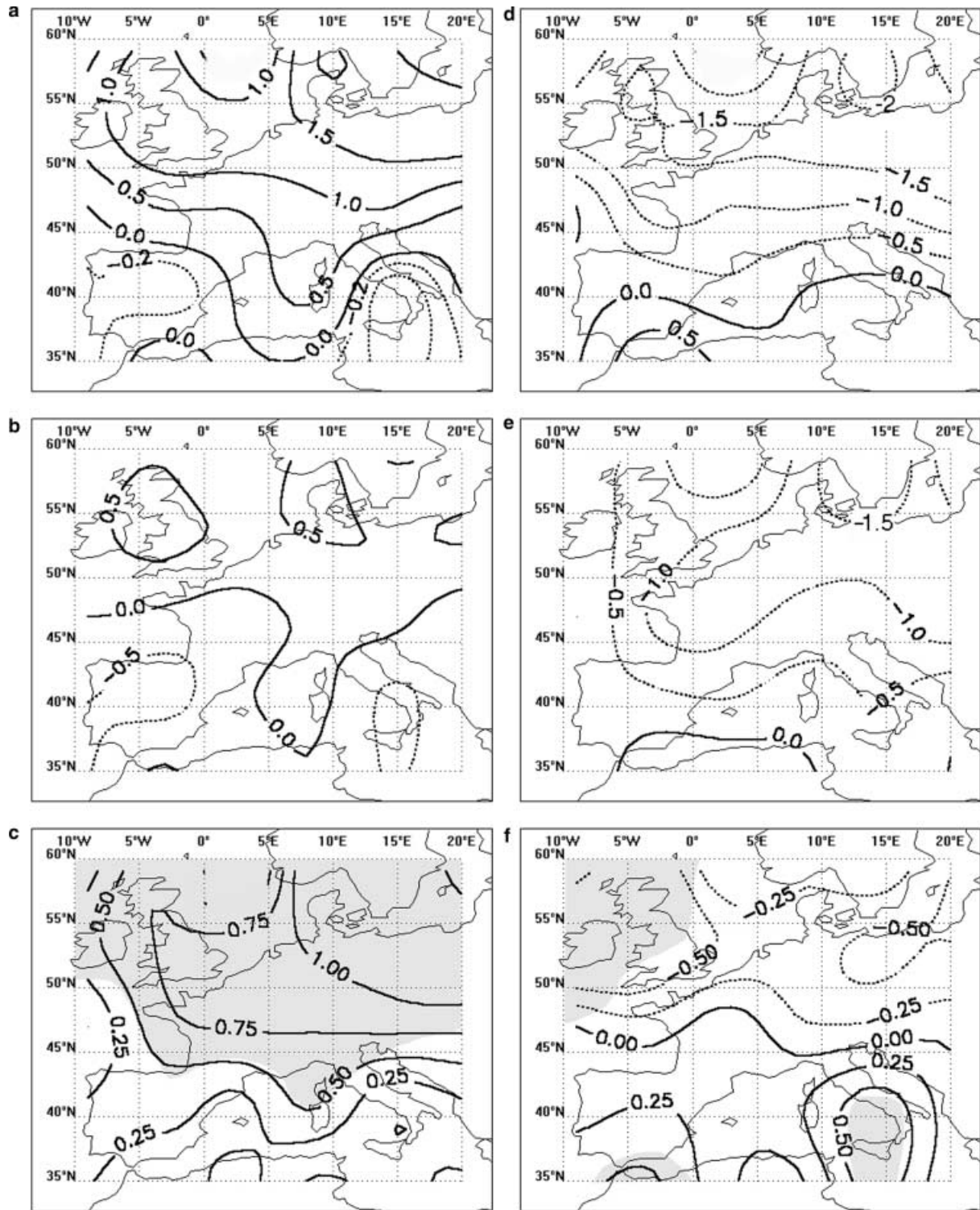


Fig. 6 a Composite of the winter averaged (DJF) land-surface temperature anomalies for years in which the NAO winter index is $NAO > 1.5$. *Continuous line* indicates positive or zero anomalies and *dotted line* indicates negative anomalies. Units are °C. Contour interval is 0.5 °C for positive anomalies and 0.2 °C for negative anomalies. **b** As in a but for years in $0 < NAO \leq 1.5$; contour

interval is 0.5 °C both for negative and positive anomalies. **c** Difference a minus b; contour interval is 0.25 °C. *Shading* indicates local statistical significance of the difference at 95%. **d** As in a but for $NAO < -1.5$; contour interval is 0.5 °C **e** As in a but for years in which $-1.5 < NAO \leq 0$; contour interval is 0.5 °C. **f** as in c but for the difference d minus e; contour interval is 0.25 °C

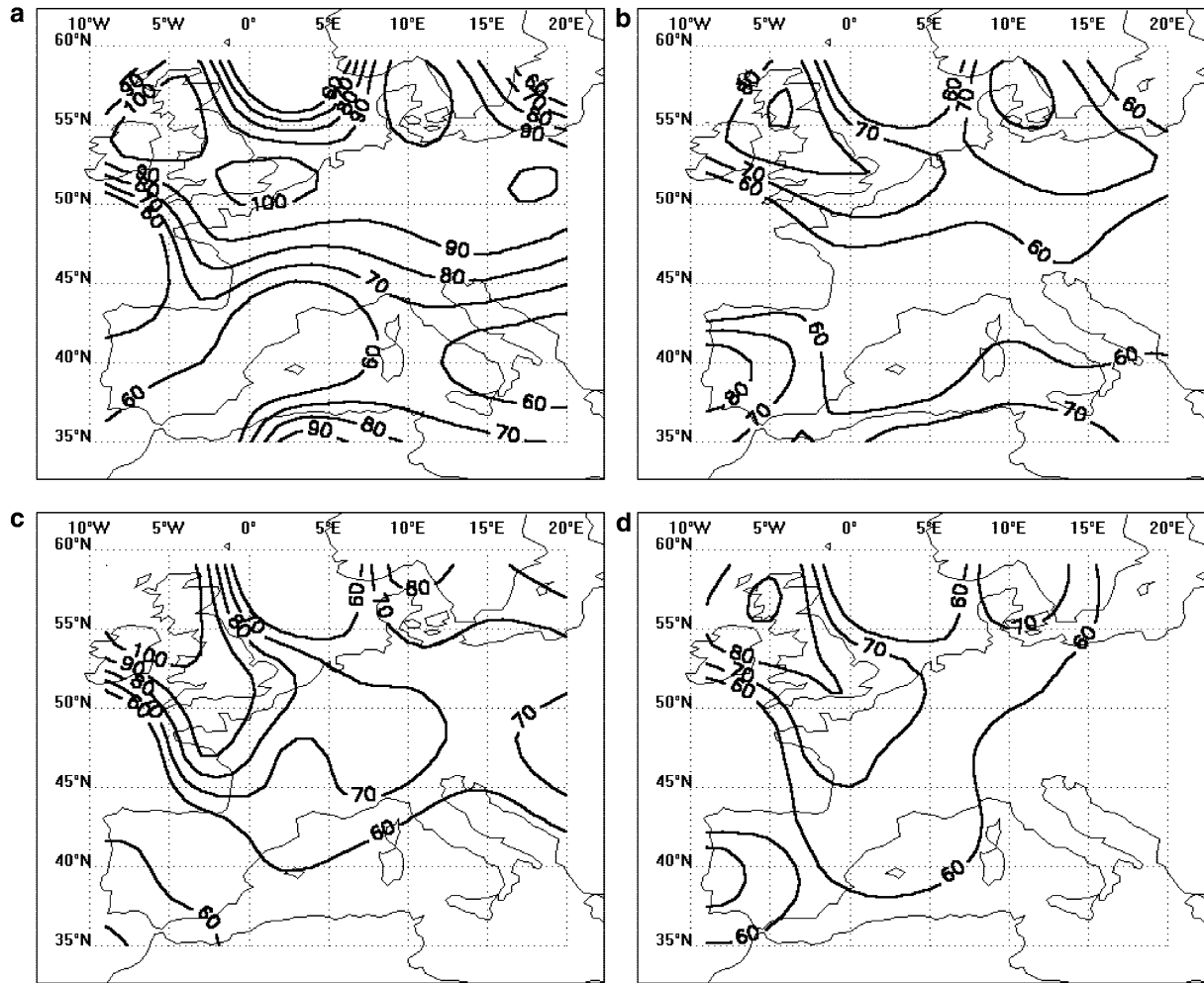


Fig. 7a–d Percentage of consistent signals in the relationship between the NAO and temperatures. The values are the percentage of events having a temperature anomaly of the same sign that the composite

anomaly. **a** Shows the results for extremely positive NAO index, **b** for moderately positive, **c** for extremely negative and **d** for moderately negative. Contour interval is 10%, ranging from 60% to 100%

(in agreement with the results of composite analysis). This suggests that over this area, a large percent of temperature anomalies during winters with extremely and moderately positive NAO index are strongly negative, but some slightly positive anomalies can be found.

Overall Fig. 7 shows that the relationship between NAO and temperatures has different characteristics in different parts of the studied area. Temperatures over the British Isles and southern Scandinavia are always influenced by the NAO state, presenting maximum positive values of the anomalies during positive extremes of the NAO and maximum negatives anomalies when negative extremes of the NAO occur. Osborn et al. (1999) and Hurrell and van Loon (1997) have also found these regions to be especially sensitive to the NAO. Other areas, like Central Europe, are scarcely influenced by the NAO during moderately positive NAO winters. Areas such as the Iberian Peninsula seem to be more influenced by moderately positive than by extremely positive NAO events.

4.3.2 Analysis of the periods: 1875–1939 and 1940–1997

Section 4.2.1 showed the spectral behaviour of the NAO to be highly non-stationary. The possible dependence of spatial patterns of temperature in Europe on the NAO spectral characteristics is analysed in this section. To study this dependence, we divided the data in two different subsets, the first one from 1875 to 1939 (first subset hereafter) and the second one from 1940 to 1997 (second subset hereafter). A PCA was carried out independently on both subsets. The spectral behaviour of the NAO winter index in these two periods is quite different. While in the period 1875–1939 the spectra of the NAO closely resembles that of a white-noise process, the period 1940–1997 is characterised, mainly from 1960 onwards, by a strong oscillation with period between 6 and 10 years. Thus, the analysis of these two subsets highlights possible differences in the behaviour of the temperatures associated with changes in the spectral behaviour of the NAO.

Three EOFs, found to be significant for both subsets, were rotated. As shown in Fig. 8, the spatial patterns associated with the REOFs are similar. In the analysis of both subsets, the leading mode of variability proves to be one that resembles the NAO signature in the tem-

peratures (Figs. 8a, d). Both patterns are alike and also similar to the pattern in Fig. 1a. The correlation between the winter NAO index and the PC series is 0.72 for the first subset and 0.82 for the second. The explained variance is 37% and 43.9% for the first and second

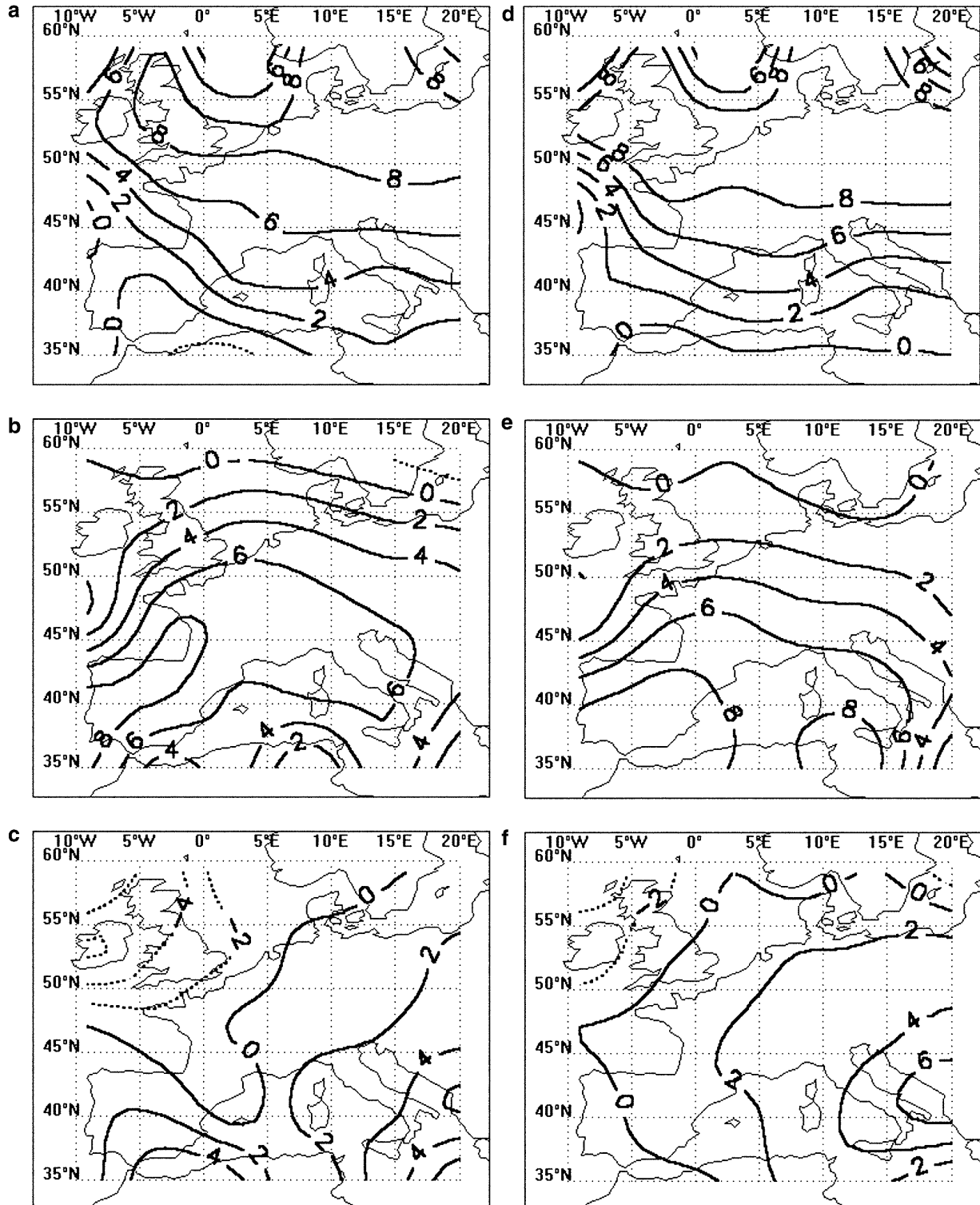


Fig. 8a–f Loading factors (by ten) for the a first, b second and c third REOF resulting from the analysis of the winter temperatures data subset 1875–1939; and d first, e second and f third REOF resulting from the analysis of the subset 1940–1997

subsets, respectively. The main differences between the two patterns are the slightly higher values of the loading factors over Southern Europe (especially in the Iberian Peninsula) in the second subset compared with the first one. The second REOF explains 28% of the variability in the two subsets, and the spatial modes (Fig. 8b, e) are alike and also similar to the second mode found in the analysis of the entire data set (Fig. 1b). The third REOF (Fig. 8c, f) explains 10% and 9% of the variability of the first and second subset, respectively. The patterns show a certain mixing of those in Fig. 1c, d. It could be concluded that during periods in which NAO index is characterised by markedly different spectra the spatial patterns of variability are substantially the same. This suggests that the spatial patterns of temperature in the study area are independent of the NAO spectra. The same behaviour is found by Werner and von Storch (1993).

5 Summary and conclusion

The relationship between European winter temperature spatial and temporal modes of variability and the North Atlantic Oscillation has been analysed for the period 1852–1997.

A PCA shows that the most important mode of spatial variability of the winter temperatures (38.1% explained variance) can be identified with the NAO. The mode is representative mainly of the variability of Western and Central Europe, southern Scandinavia and the British Isles. Variability of the temperatures in Southern Europe is better represented by the second mode.

Temporal modes of variability of the winter NAO index and temperatures were studied using wavelet analysis. Results show that the NAO index presents a strong non-stationary behaviour. There is no evidence for a single persistent temporal mode of temporal variability within the time interval 1826–1997. Power is concentrated mainly in periods of less than 10 years. The most important feature is a quasi-periodic oscillation, with a period in the band of 6–10 years and maximum amplitude at 8 years, during the periods 1842–1868 and 1964–1994. In the band of 4–6 years, valuable power was found in the periods 1857–1875, 1939–1946 and 1956–1966. A quasi-biennial oscillation dominated during the period 1880–1890. Between 1875 and 1940, the spectrum of the NAO is almost white. Overall, wavelet analysis shows an increase in the importance of the low-frequency signal in the NAO index in the latter part of the twentieth century compared with the first part of this century, but not compared with the period 1840–70.

An analysis of the relationship between the occurrence of extreme events of the NAO and its spectral behaviour has been made. The comparison of the number of extreme values (positive or negative) of the NAO index during 1875–1939 (in which spectral behaviour of NAO resembles white noise) and during 1940–1997 (in which oscillations in the band of 6–10 years

period predominate) shows no significant differences. This suggests that quasi-periodic oscillations in the NAO do not lead to more extreme episodes. Rather, this signifies only that persistence in an extreme value of the oscillation for few years is more likely. These episodes of persistence can be found, for instance, in the periods 1973–1975, 1983–1984 and also between 1989–1995, with five of the seven winters having a value of the NAO > 1.5. Similar episodes of persistence can also be found from 1853 to 1856.

Wavelet analysis of the PC series of the period 1852–1997 indicates that the leading mode has a similar non-stationary spectral behaviour to those of the NAO. Particularly energetic modes of coherent variability between the leading temperature PC series and the NAO index can be found in the band of 2–6 year periods for 1857–1879 and 1978–1984, and between 6–10 years from 1961 to 1991. The PC series associated with the second REOF (representative mainly of southwestern Europe) shows a low-frequency oscillation of 15-year periods, between 1878 and 1901.

The possible dependence of spatial patterns of temperature in Europe on the NAO spectral characteristics has been analysed by carrying out two independent PCAs for the periods 1875–1939 and 1940–1997. Results show that during these two periods, in which the NAO index has very different spectral characteristics, the spatial patterns of variability are substantially the same. This suggests that the spatial patterns of variability of temperature are independent of the NAO spectra.

The relationship between the NAO and the temperature variability in Europe as a function of the state of the oscillation has been studied using composites of temperatures based on the value of the NAO index. Consistency among events of this relationship has also been examined. Overall, results show that the relationship between NAO and temperatures has different characteristics in different parts of the studied area. There are areas, e.g. the British Isles and southern Scandinavia, in which temperatures are always influenced by the NAO state. Furthermore, these areas present the maximum anomalies associated with both positive (anomalies are around 1.5 °C) and the negative (anomalies are between –1.5 and –2 °C) extremes of the NAO, and high coherence in all the phases and intensities of the NAO. Over these areas, thus, the relationship between NAO and temperatures seems to be linear to the highest degree. Other areas, such as Central Europe, are scarcely influenced by the NAO during the moderately positive phase (anomalies less than 0.5 °C and coherence 60%–70%). During the extremely positive phase, influence of the NAO in this region is substantially greater (anomalies of 1–1.5 °C and coherence around 90%). Furthermore, only small changes both in temperature and in percent of coherence are found over this area when extremely negative and moderately negative NAO are considered (temperature anomalies are between –1 and –1.5 °C and coherence between 60 and 70%). Areas such as the Iberian Peninsula seem to be

more influenced by moderately positive (anomalies -0.5°C and coherence 60–80%) than by extremely positive NAO (anomalies around -0.2°C and coherence 60%).

This empirical evidence suggests that winter temperatures in most part of the study area do not vary in a linear way with respect to phase and intensity of the NAO. Sampling, especially in the cases of negative NAO index, can influence results. Due to the sampling, the patterns found are somewhat of a blend between a forced signal due to the NAO and climate noise, the latter being independent of the state of the NAO. Interpretations of the results are difficult to make solely on the basis of the data used. Further research is needed to confirm such non-linearity. Regarding the spectral behaviour of the NAO index, and although internally generated atmospheric conditions have been proposed to produce interdecadal variability in the NAO (e.g. Perlwitz and Graf 1995), low-frequency variability (interdecadal and longer) in the NAO have recently been associated with processes involving the ocean (Rodwell et al. 1999; Taylor and Stephens 1998; Rajagopalan et al. 1998; Timmermann et al. 1998). In a forthcoming work, this analysis will be completed, including other data such as sea surface temperature, sea-level pressure and geopotential height. The inclusion of these data will enable the exploration of a physical and dynamical interpretation of the observational results.

Acknowledgements The Spanish CICYT, Project CLI98-0930-C02-01 financed this study. We would like to thank Dr. Phil Jones (Climatic Research Unit, University of East Anglia, UK) for providing the data used. We are very grateful to Ricardo Machado Trigo (Climatic Research Unit, University of East Anglia, UK) for useful comments and suggestions. We also want to thank Professor J.M. Angulo (Statistics Department of the University of Granada) very much for valuable discussions concerning the statistical procedures used in this work. Wavelet software was provided by C. Torrence and G. Compo and is available at: URL: <http://paos.colorado.edu/research/wavelets/>. The comments of two anonymous reviewers helped to substantially improve the manuscript.

References

- Appenzeller C, Stocker TF, Anklin M (1998) North Atlantic oscillation dynamics recorded in Greenland ice cores. *Science* 282: 446–450
- Barnston AG, Livezey RE (1987) Classification, seasonality and persistence of low-frequency atmospheric circulation patterns. *Mon Weather Rev* 115: 1083–1126
- Canovos GC (1988) Probabilidad y Estadística. Aplicaciones y métodos. McGraw-Hill, Mexico, 651 p
- Cheng X, Nitshe G, Wallace JM (1995) Robustness of low-frequency circulation patterns derived from EOF rotated analysis. *J Clim* 8: 1709–1713
- Esteba-Parra MJ (1995) Contribución al estudio de la evolución del clima de España en el periodo Instrumental. PhD Thesis, University of Granada, Spain, 420 p
- Foufoula-Georgiou E, Kumar P (1995) Wavelets in geophysics. Academic Press, London, 373 p
- Hoerling MP, Kumar A, Zhong M (1997) El Niño, La Niña, and the nonlinearity of their teleconnections. *J Clim* 10: 1769–1787
- Huang J, Higuchi K, Shabbar A (1998) The relationship between the North Atlantic Oscillation and El Niño-Southern Oscillation. *Geophys Res Lett* 25: 2707–2710
- Hurrell JW (1995) Decadal trends in North Atlantic Oscillation and relationship to regional temperature and precipitation. *Science* 269: 676–679
- Hurrell JW (1996) Influence of variations in extratropical wintertime teleconnections on Northern Hemisphere temperatures. *Geophys Res Lett* 23: 665–668
- Hurrell JW, van Loon H (1997) Decadal variations in climate associated with the North Atlantic Oscillation. *Clim Change* 36: 301–326
- Jones PD (1994) Hemispheric surface air temperature variations: a reanalysis and an update to 1993. *J Clim* 7: 1794–1802
- Jones PD, Osborn TJ, Briffa KR (1997a) Estimating-sampling errors in large-scale temperature average. *J Clim* 10: 2548–2568
- Jones PD, Jonsson T, Wheeler D (1997b) Extension to the north Atlantic Oscillation index using early instrumental pressure observations from Gibraltar and southwest Iceland. *Int J Climatol* 17: 1–18
- Kaiser G (1994) A friendly guide to wavelets. Birkhäuser, Boston, 296 p
- Kiladis N, Diaz HF (1989) Global climatic anomalies associated with extremes of the Southern Oscillation. *J Clim* 2: 1069–1090
- Lau KM, Weng HY (1995) Climate signal detection using wavelet transform: How to make a time series sing. *Bull Am Meteorol Soc* 76: 2391–2402
- Lorenz EN (1997) The essence of chaos. University of Washington Press, Seattle, USA, 227 p
- Mächel H, Kapala A, Flohn G (1998) Behaviour of the centres of action above the Atlantic since 1881: Part I: characteristic of seasonal and interannual variability. *Int J Climatol* 18: 1–22
- Moses T, Keladis G, Diaz HF, Barry R (1987) Characteristic and frequency of reversal in mean sea level pressure in the North Atlantic sector and their relationship to long-term temperature trends. *Int J Climatol* 7: 13–30
- Nicholls N, Gruza GV, Jouzel J, Karl TR, Ogallo LA, Parker DE (1996) Observed climate variability and change. In: Houghton JT, Meira Filho LG, Callander BA, Harris N, Kattenberg A, Maskell K (eds) *Climate Change 1995: The IPCC Second Assessment*. Cambridge University Press, Cambridge, UK, pp 133–192
- North GR, Bell TL, Cahalan RF, Moeng FJ (1982) Sampling errors in the estimation of empirical orthogonal functions. *Mon Weather Rev* 110: 699–706
- Osborn TJ, Briffa K, Tett SFB, Jones PD, Trigo RM (1999) Evaluation of the North Atlantic Oscillation as simulated by a climate model. *Clim Dyn* 15: 685–702
- Palecki MA, Leathers DJ (1993) Northern Hemisphere extratropical circulation anomalies and recent January land surface temperature trends. *Geophys Res Lett* 9: 819–822
- Parker DE, Jones PD, Bevan A, Folland CK (1994) Interdecadal changes of surface temperature since the late 19th century. *J Geophys Res* 99: 14 373–14 399
- Percival DP (1995) On estimation of the wavelet variance. *Biometrika* 82: 619–631
- Perlwitz J, Graf HF (1995) The statistical connection between tropospheric and stratospheric circulation of the Northern Hemisphere in winter. *J Clim* 8: 2281–2295
- Pettit AN (1979) A non-parametric approach to the change point problem. *Appl Stat* 28: 126–135
- Pozo-Vázquez D, Esteban-Parra MJ, Rodrigo FS, Castro-Diez Y (2000) An analysis of the variability of the North Atlantic Oscillation in the time and the frequency domains. *Int J Climatol* (In press)
- Preisendorfer RW (1988) Principal components analysis in meteorology and oceanography. Elsevier, Amsterdam, 419 p
- Rajagopalan B, Kushnir Y, Tourre YM (1998) Observed decadal midlatitude and tropical Atlantic variability. *Geophys Res Lett* 25: 3967–3970
- Richman MB (1986) Rotation of principal components. *J Climatol* 6: 293–335

- Rodwell MJ, Rowell DP, Folland CF (1999) Oceanic forcing of the wintertime North Atlantic Oscillation and European climate. *Nature* 398: 320–323
- Rogers JC (1984) The association between the North Atlantic Oscillation and the Southern Oscillation in the Northern Hemisphere. *Mon Weather Rev* 112: 1999–2015
- Rogers JC, van Loon H (1979) The seesaw in winter temperatures between Greenland and Northern Europe Part II: some oceanic and atmospheric effects in middle and high latitudes. *Mon Weather Rev* 107: 509–519
- Ropelewski CF, Jones PD (1987) An extension of the Tahiti-Darwin Southern Oscillation Index. *Mon Weather Rev* 115: 2161–2165
- Sneyers ET (1992) On the use of statistical analysis for the objective determination of climate change. *Meteorol Z* 1: 247–256
- Taylor AH, Stephens JA (1998) The North Atlantic Oscillation and the latitude of the Gulf-Stream. *Tellus A* 50: 134–142
- Timmermann A, Latif M, Voss R, Grötzner A (1998) Northern Hemispheric interdecadal variability: a coupled air-sea mode. *J Clim* 8: 1906–1931
- Torrence C, Compo G (1998) A practical guide to wavelet analysis. *Bull Am Meteorol Soc* 79: 61–78
- Trenberth K (1990) Recent observed interdecadal climate changes in the Northern Hemisphere. *Bull Am Meteorol Soc* 71: 988–993
- Trenberth K (1995) Atmospheric circulation climate changes. *Clim Change* 31: 427–453
- Trenberth KE (1984) Signal versus noise in the Southern Oscillation. *Mon Weather Rev* 112: 327–333
- van Loon H, Rogers JC (1978) The seesaw in winter temperatures between Greenland and Northern Europe Part I: general description. *Mon Weather Rev* 106: 296–310
- von Storch H (1995) Spatial patterns: EOFs and CCA. In: von Storch H, Navarra A (eds) *In: Analysis of climate variability applications of statistical techniques* Springer, Berlin Heidelberg, pp 227–257
- Wallace JM, Gutzler DS (1981) Teleconnections in the geopotential height field during the Northern Hemisphere winter. *Mon Weather Rev* 109: 784–812
- Wallace JM, Zhang Y, Bajuk L (1996) Interpretation of interdecadal trends in Northern Hemisphere surface air temperature. *J Clim* 9: 249–259
- Wallace JM, Zhang Y, Renwick JA (1995) Dynamical contribution to hemispheric temperature trends. *Science* 270: 780–783
- Wang B, Wang Y (1996) Temporal structure of the Southern Oscillation as revealed by waveform and wavelet analysis. *J Clim* 9: 1586–1598
- Werner P, von Storch H (1993) Interannual variability of Central European mean temperature in January/February and its relation to the large-scale circulation. *Clim Res.* 3: 195–207
- Yiou P, Baert E, Loutre MF (1996) Spectral analysis of climate data. *Surv Geophys* 17: 619–663
- Zorita E, von Storch H (1997) A survey of statistical downscaling techniques. GKSS report GKSS/E/20, Hamburg, 42 p